RESEARCH ARTICLE

A 3D Skeleton Points-Based Hierarchical Body Modeling Approach for Intelligent Online Clothing Fitting Systems

HUAPING ZHU[1], TAO ZHANG[2], AND FEN WANG[ID][3]
[1]College of Art and Design, Nanning Normal University, Nanning 530001, China
[2]Shenzhen Shanglong Technology Company Ltd., Shenzhen 518000, China
[3]College of Humanities, Arts and Design, Guangxi University of Science and Technology, Liuzhou 545000, China

Corresponding author: Fen Wang (qinyusheji2020@163.com)

ABSTRACT The online clothing fitting (OCF) has been a prevalent Internet application. It utilizes multimedia processing algorithms to generate clothing fitting effect images for consumers in virtual way. Existing related works mainly neglected the diverse skeleton structure characteristics of different users, which limits generalization of OCF systems. To handle such challenge, this paper proposes a novel 3D skeleton points-based hierarchical body modeling approach for intelligent OCF systems. Specifically, it focuses on two types of posture features, integrates circumferential features of body, and distinguishes the trunks and the limbs. Then, a global-local singular value decomposition algorithm is designed to hierarchically control the deformation of 3D skeleton format cooperatively, in order to optimize the fitting results. Finally, we conduct some experimental evaluation through computer programming to verify efficiency of the proposal. The results show that relative tracking error of the new method is reduced by about 10%, and the real-time tracking accuracy between the clothing fitting results and the human body is obviously improved.

INDEX TERMS 3D skeleton modeling, hierarchical body modeling, intelligent systems, singular value decomposition.

I. INTRODUCTION

With the improvement of people's living standards, the demand for high-quality and personalized modern fashion has promoted the development of the clothing customization industry [1]. At the same time, online shopping has changed people's consumption patterns. The most obvious difference between online consumption of clothing and offline store purchases is that customers lack the personalized experience and real-time interaction of clothing fitting when purchasing online, and the customer's own sense of experience and suitability are important factors that promote purchase intentions [2], [3].

Nowadays, with the rapid development of information technologies such as 5G communication, artificial intelligence AI, and the Internet of Things (IoT), especially the close integration of 5G high-definition video communication

The associate editor coordinating the review of this manuscript and approving it for publication was Siddhartha Bhattacharyya[ID].

network, AR/VR virtual technology and the clothing industry, it has entered the clothing virtual clothing fitting system [4]. Development, by providing a personalized virtual clothing model to fit on the human body, the function of convenient clothing fitting is realized, and the experience of the fitting process is improved to a certain extent.

The existing virtual clothing fitting technologies can be generally divided into two types: two-dimensional plane-based and three-dimensional space-based [5]. The method based on two-dimensional plane is completed by transforming the pose feature of two-dimensional clothing pictures, but this method lacks the three-dimensional effect of trying on. In the clothing manufacturing process, a 3D volume scanner is used to collect all human body size data, and combined with the 3D clothing EDA simulation tool to show the three-dimensional fitting effect, with high precision, but expensive equipment and low efficiency [6].

The 3D virtual fitting system can be divided into two categories. One uses a virtual mannequin based on high-precision
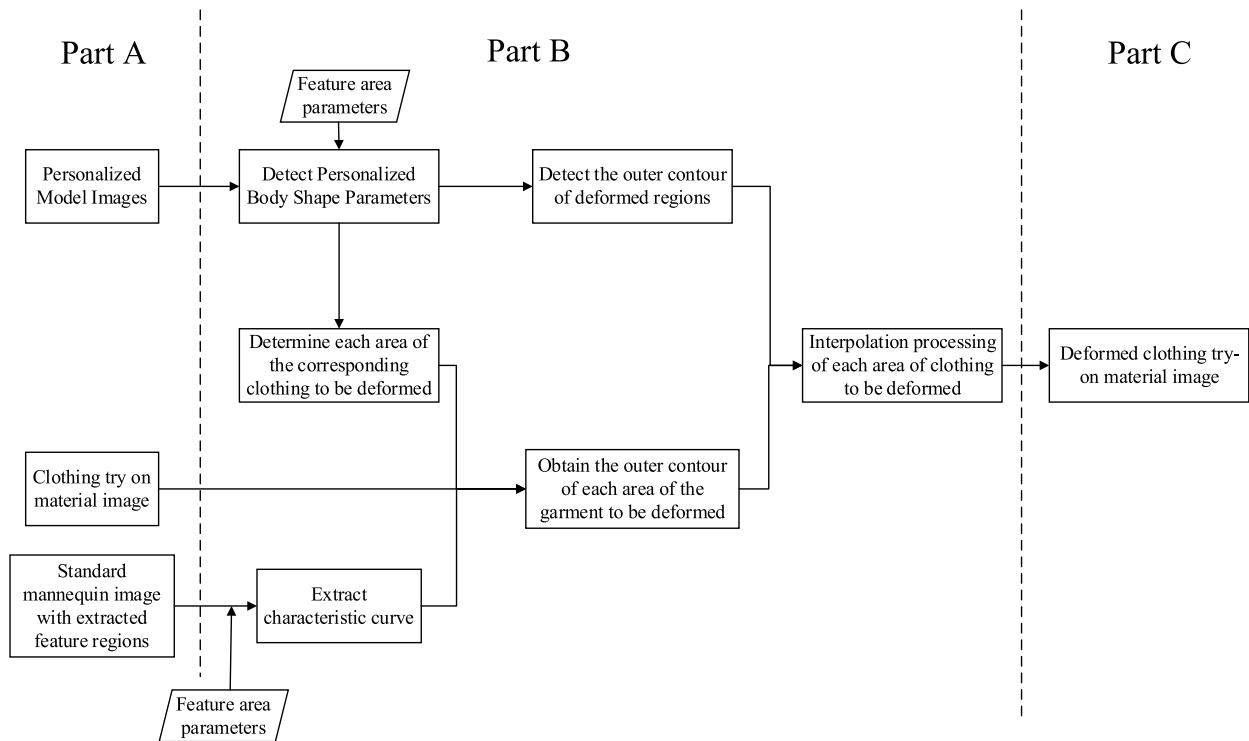
FIGURE 1. The framework of the clothing inference deformation algorithm.

data modeling to perform virtual fitting on clothing. Representative products such as: Fitiquette in India, and virtual fitting mirrors developed by FaceCake Marketing Technologies in the United States [7], the Maxi somatosensory mirror of the domestic modern avenue company, etc. The above product maps a 3D garment model onto an avatar. Cucchi et al. Extract real user facial avatars and combine them with 3D virtual mannequins [8]. However, the tracking method of point-by-point assignment of virtual human body model-clothing model has low efficiency, large amount of data processing and poor realism.

The other uses Microsoft Kinect somatosensory camera to realize human motion tracking and 3D virtual clothing modeling based on RGB-D (grayscale, depth) image perception data [9]. Yousef based on the Kinect human skeleton point model and iterative estimation of clothing anchor points, the modified 3D clothing model realizes the virtual clothing fitting of short skirts on the real human body.

This paper proposes to use the Kinect skeleton point model and fuse human feature data to construct a 3D clothing skeleton point hierarchical model to enhance the virtual clothing model's tracking of human motion and posture [10]. At the same time, a layered iterative GL-SVD algorithm is designed to control the overall positioning and local tracking of the 3D clothing model in the process of human motion, so as to achieve dynamic, real-time collaborative tracking and high-precision matching between the 3D clothing model and the real human body.

II. MATHEMATICAL MODELING FOR VIRTUAL CLOTHING FITTING IN 2D SCENES

In the clothing E-Commerce platform, the most basic effect to be achieved by 2D virtual clothing fitting is that when the user clicks or drags the clothing thumbnail with the mouse, the corresponding clothing fitting material image is quickly and naturally superimposed on the model image. It is guaranteed that the rest of the model image remains unchanged except for the area covered by the garment image [11], [12]. In clothing material processing for 2D virtual clothing fitting, the final clothing fitting material image has the same size as the model image, and the outside of the clothing area is set to be transparent. This sets the stage for image overlays in virtual clothing fitting.

The mathematical description of the image overlay process in 2D virtual clothing fitting can be expressed as follows:

$$R = \alpha M + (1 - \alpha)A(\alpha = 0, 1) \tag{1}$$

Among them, R represents the result image after virtual clothing fitting, M represents the undressed model image, A represents the clothing fitting material image, α is the superposition coefficient, the value is 0 or 1. It is easy to find that when $\alpha = 0$, R = A can be obtained, that is, the result image is completely reflected as the material image of clothing fitting, when $\alpha = 1$, R = M can be obtained, that is, the resulting image is completely embodied as an undressed model image. Specifically, in the 2D virtual clothing fitting, the image overlay operation is implemented according to the following strategy.

A is scanned pixel by pixel in the order from top to bottom and from left to right, and the color value of each scanned pixel is obtained. If the alpha channel value of the color of the current pixel in A is 0, set α to 1, that is, set the color of the pixel at the current position in the result image R to the color value of the pixel at the current position in the image M of the undressed model. Conversely, if the alpha channel value of the current pixel color in A is not 0, set α to 0, that is, set the color of the pixel at the current position in the result image R to the color value of the pixel at the current position in the clothing fitting material image A. Through such image overlay operation, the most basic effect of 2D virtual clothing fitting is realized.

A. APPAREL REASONING DEFORMATION ALGORITHM

The feature area of the standard model image divided according to the prior art, combined with the specific reality of the human body trying on the clothing, the deformation area of the clothing is divided into four clothing areas corresponding to the chest, waist, buttocks and shoulders [13]. Among them, the sleeve part of the garment is included in the shoulder garment deformation area. Based on the principle of image superposition in 2D virtual clothing fitting, this paper uses interpolation technology to realize the reasoning and deformation of clothing clothing fitting material images. The framework of the clothing deformation algorithm is shown in Figure 1.

In Figure 1, Part A is the input part, and the required input is the personalized body model image, the clothing fitting material image and the standard model image with the extracted feature area. Part B is the core processing part. Part C is the output part. First, the characteristic curve of the standard model image is extracted according to the relevant parameters of the divided characteristic regions. The feature area parameter is the coordinate of the feature area of the standard model image. Next, the body shape parameters in the personalized body model image are detected, and each deformed characteristic area is obtained, combined with the characteristic area parameters, the outer contour of each deformed characteristic area is detected, and each area corresponding to the garment to be deformed is determined [14], [15]. Then, according to the extracted characteristic curve, the outer contour of each area of the garment to be deformed is obtained. Finally, the outer contour of the personalized body shape and the outer contour of the clothing are compared and analyzed, and then each area of the clothing to be deformed is interpolated to obtain the deformed clothing fitting material image.

B. IMPLEMENTATION STEPS OF CLOTHING REASONING DEFORMATION

1) IMAGE FEATURE CURVE EXTRACTION

The extraction object of the characteristic curve is the standard model image. The main purpose of extracting the characteristic curve is to obtain the outer contour of each area to be deformed in the clothing fitting material image
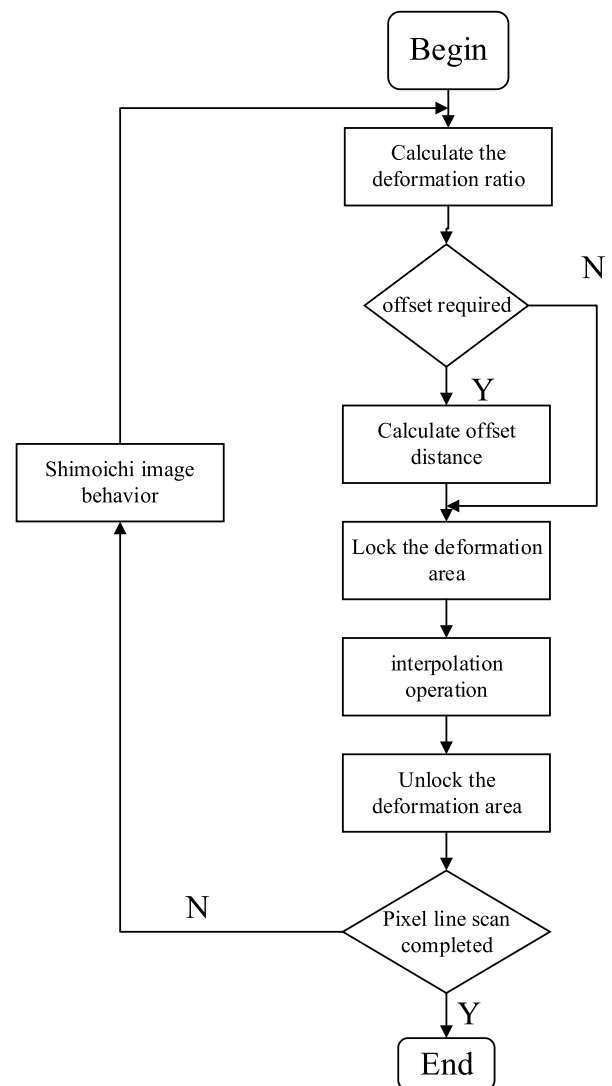

FIGURE 2. The core flow chart of the clothing reasoning deformation algorithm.

efficiently and accurately [16], [17]. Due to the diversity and complexity of the outer contours of the clothing fitting material images and the fact that the regions to be deformed in the clothing fitting material images are mainly based on personalized body models, traditional edge detection and region growth methods are difficult to obtain effectively.

2) OUTER CONTOUR OF THE CLOTHING AREA TO BE DEFORMED

The acquisition of the outer contour of each area to be deformed in the clothing fitting material image is carried out in the following two steps: the first step is to determine each area to be deformed in the clothing fitting material image. Taking the personalized body shape model image as the detection object, the four personalized body shape parameter values of bust, waist, hip and shoulder width are detected, and compared with the standard model body shape

parameters [18]. The corresponding area is determined as the area to be deformed.

In the second step, the outer contour of each area to be deformed in the clothing fitting material image is obtained according to the determined characteristic curve [19]. The main idea is: for each area to be deformed in the clothing fitting material image, within the range of the corresponding standard model image feature area, starting from the determined characteristic curve, from top to bottom to the edge of the clothing fitting material image line by line Scan until the edge non-transparent pixels of each row of each area of the clothing fitting material image to be deformed are detected [20]. These edge non-transparent pixels constitute the outer contour of each area to be deformed in the clothing fitting material image.

If p and p' are the outer contour of the waist area of the clothing fitting material image to be obtained, and q and q' represent the detection route and direction. Within the range of the waist circumference control area of the standard model image, starting from the characteristic curve, scan pixel by pixel according to the route indicated by q and q' from top to bottom, until the outer contours p and p' of the waist circumference area of the clothing fitting material image are detected. The acquisition of the outer contours of other to-be-deformed regions in the clothing fitting material image is similar.

3) DEFORMATION OF CLOTHING REASONING BASED ON PERSONALIZED BODY SHAPE

Before performing deformation processing on each area to be deformed in the clothing fitting material image, it is first necessary to obtain the outer contour of each deformed area of the personalized body model image. The specific implementation method is as follows: Detecting 4 personalized body shape parameter values of bust, waist, hip and shoulder width, and comparing with the standard model body shape parameters [21]. Then binarize the feature area of the personalized body model image, and then performs edge detection constrained by the boundary of the feature region to obtain the outer contour of the deformed region.

After the outer contours of the deformed regions of the personalized body model image and the outer contours of the regions to be deformed in the clothing fitting material image are obtained, the deformation processing can be performed on the regions to be deformed in the clothing fitting material image. Because in the 2D personalized body shape customization, the personalized body shape when the bust, waist, hip and shoulder width increase is the most common, so the clothing deformation in this case is the most typical. This paper focuses on this typical clothing deformation [22]. Figure 2 shows the core flow of the clothing reasoning deformation algorithm.

In a specific implementation, it is performed from top to bottom in pixel row units. First, the abscissa of the current pixel row is extracted from the deformed area of the

personalized body model image and the outer contour of the to-be-deformed area of the corresponding clothing fitting material image, and then it is determined whether the deformation operation needs to be performed. Let x_1 and x_2 be the left and right abscissas of the current pixel row in the deformed area of the personalized body model image, respectively, and x_3 and x_4 are the left and right abscissas of the current pixel row in the to-be-deformed area of the corresponding clothing fitting material image, respectively.

W_{source}, $W_{destination}$ represent the initial width and the deformed width of the current pixel row in the to-be-deformed area of the clothing fitting material image, respectively, and R represents the deformation ratio, which refers to the ratio of the deformed width to the initial width of the current pixel row in the to-be-deformed area of the clothing fitting material image, that is, $W_{destination}/W_{source}$, D represents the offset distance, which refers to the distance that the current pixel row in the to-be-deformed area of the clothing fitting material image needs to be translated with its geometric center as the coordinate origin. If the deformation condition $x_1 < x_3$ or $x_2 > x_4$ is satisfied, the deformation operation is performed. In the deformation operation, the calculation of the deformation ratio R and the offset distance D is extremely critical. Typical situations are divided into the following three types:
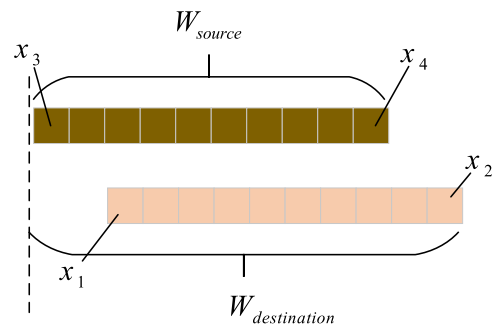

FIGURE 3. Diagram of garment deformation 1.

Case 1: $x_1 \geq x_3$ and $x_2 > x_4$ holds, as shown in Figure 3. Among them, the yellow square represents the current pixel row in the deformed area of the personalized body model image, and the purple square represents the current pixel row in the to-be-deformed area of the clothing fitting material image. R and D are calculated as:

$$\begin{cases} R = \dfrac{W_{destination}}{W_{source}} = (x_2 - x_3 + 1.0)/(x_4 - x_3 + 1.0) \\ D = \dfrac{x_2 + x_3}{2} - \dfrac{x_4 + x_3}{2} = (x_2 - x_4)/2 \end{cases}$$

(2)

In this case, the right skin area of the personalized body model image extends beyond the right edge of the clothing fitting footage image. The basic idea of clothing deformation is: take the left border of the current pixel row of the to-be-deformed area of the clothing fitting material image as the benchmark,

and stretch the current pixel row of the to-be-deformed area of the clothing fitting material image to the right until it covers the current pixel row of the deformed area of the personalized body model image.

Case 2: $x_1 < x_3$ and $x_2 \leq x_4$ holds, as shown in Figure 4. R and D are calculated as:

$$\begin{cases} R = \dfrac{W_{destination}}{W_{source}} = (x_4 - x_1 + 1.0)/(x_4 - x_3 + 1.0) \\ D = \dfrac{x_4 + x_1}{2} - \dfrac{x_4 + x_3}{2} = (x_1 - x_4)/2 \end{cases} \tag{3}$$

In this case, the left skin area of the personalized body model image extends beyond the left edge of the clothing fitting footage image. The basic idea of clothing deformation is: Taking the right border of the current pixel row of the to-be-deformed area of the clothing fitting material image as a benchmark, stretch the current pixel row of the to-be-deformed area of the clothing fitting material image to the left until it covers the current pixel row of the deformed area of the personalized body model image.
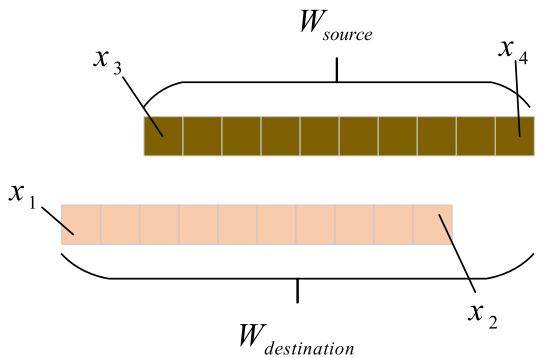

FIGURE 4. Diagram of garment deformation 2.

Case 3: $x_1 < x_3$ and $x_2 > x_4$ holds, as shown in Figure 5 (a) and (b). R and D are calculated as:

$$\begin{cases} R = \dfrac{W_{destination}}{W_{source}} = (x_2 - x_1 + 1.0)/(x_4 - x_3 + 1.0) \\ D = \dfrac{x_2 + x_1}{2} - \dfrac{x_4 + x_3}{2} = (x_1 - x_4)/2 \end{cases} \tag{4}$$

In this case, both the left and right skin regions of the personalized body model image extend beyond the corresponding left and right edges of the clothing fitting material image. The basic idea of clothing deformation is to stretch the current pixel row of the to-be-deformed area of the clothing fitting material image to the left and right ends simultaneously until it covers the current pixel row of the deformed area of the personalized body model image.

After the calculation of the deformation ratio R and the offset distance D is completed, the bilinear interpolation operation can be performed by locking the memory. Take the clothing fitting material image as the input image and

its copy as the output image. Lock the current pixel row and the adjacent next pixel row of the area to be deformed in the input and output images into the system memory, and then scan the current pixel row of the area to be deformed in the output image pixel by pixel in the order from left to right. pixel, take the geometric center of the current pixel row of the output image to be deformed as the coordinate origin to perform coordinate transformation, obtain the coordinates of the input image according to the inverse mapping method, and then calculate the color value of the pixel in the output image according to the bilinear interpolation formula. After the scanning of the current pixel row in the area to be deformed of the output image is completed, the interpolation operation of the current pixel row is completed, and the system memory is unlocked. Then, go to the next pixel row, and repeat the above operations until the deformation of the to-be-deformed area of the clothing fitting material image is completed.

III. 3D CLOTHING SKELETON POINTS-BASED HIERARCHICAL BODY MODELING

Human movement mainly drives the movement of the trunk and the linkage of the limbs through the spine and joints. In this paper, the spine, trunk and limbs are used to distinguish the motion characteristics of the overall and local bone points in order to more accurately match the complex characteristics of human body posture changes [23]. Based on this, the three-dimensional clothing bone points are established. Layered model. In the process of human body movement, the dynamic matching relationship between the clothing skeleton point features and the human body skeleton point features can be maintained, so that the clothing model can follow the human body to perform overall positioning and local changes.

Based on the human skeleton model data collected by the Kinect somatosensory device, it is defined that the set of human dynamic feature points $X\{X_1, X_2\}$ includes two subsets. Among them, the subset X_1 (red) is the overall dynamic feature point set of the human body, including: left shoulder, right shoulder, spine center, left hip bone, right hip bone, hip bone center and other joints. X_2 (green) is a set of local dynamic feature points of the human body, including joints such as left elbow, right elbow, left wrist, right wrist, left knee, right knee, left ankle, and right ankle. Similarly, the clothing dynamic feature point set $Y\{Y_1, Y_2\}$. Among them, the subset Y_1 (red) is the overall dynamic feature point set of the clothing, and Y_2 (green) is the local dynamic feature point set of the clothing.

At the same time, the body circumference size can be calculated and fitted according to the ellipse model of the human body section and the data sensed by the Kinect somatosensory device. The formula for calculating the circumference of the human body, that is, the circumference of the ellipse is as follows:

$$L = 2\pi\sqrt{\frac{a^2 + b^2}{2}} \tag{5}$$

TABLE 1. Personalized human circumference feature.

Gender	Chest Circumference/cm	Waistline Hip/cm	Circumference Thigh/cm	Circumference/cm
Male	93	84	88	34
Female	86	72	85	28

In the formula, L is the perimeter of the ellipse, a and b are the semi-major and semi-minor axes of the ellipse. Based on the human body information RGB and other characteristic data collected by Kinect, the semi-major axis a and semi-minor axis b of the ellipse can be obtained by traversing the pixel points of the girth section. Table 1 shows an example of the calculation data of the circumference feature of a single male and female model in the experiment.

(a) the case of $x_2 - x_4 \geq x_3 - x_1$

(b) the case of $x_2 - x_4 < x_3 - x_1$

FIGURE 5. Diagram of garment deformation 2.

IV. COLLABORATIVE TRACKING OF 3D DYNAMIC CLOTHING FEATURES

In the process of human motion, the deformation control of the 3D clothing model is embodied in the spatial position change tracking of feature points Y and X, as well as the telescopic deformation tracking of the associated motion vector between the feature points [24]. Therefore, the idea of dynamic feature collaborative tracking in this paper includes two aspects: First, the positioning and tracking of the global and local feature points, and the second, the synchronous scaling and rotation of the associated motion vector. In partic-

ular, this paper proposes a GL-SVD decomposition algorithm based on global-local iterative hierarchical fitting to optimize the accuracy and real-time performance of collaborative tracking during motion [25]. Finally, quaternions and human depth features are used to control the transformation of the associated vectors.

A. OVERALL POSITIONING OF CLOTHING

In three-dimensional space, the coordinate registration between two points set can be expressed as a transformation of rotation and translation, that is, it is realized by using rotation and translation matrices. The coordinates of the feature points are extracted from X_1 and Y_1 to construct matrices A and B, which represent the overall dynamic feature point coordinates of the human body and clothing, respectively. The transformation of matrix B to A can be expressed as the following transformation formula:

$$A = R \times B + T \tag{6}$$

In the formula: R is the rotation matrix; T is the translation matrix. Through the above transformation formula, the matrix B and A have established a corresponding relationship, and B can be transformed into A.

In this paper, the R and T matrices are solved by performing singular value decomposition (SVD) on the covariance matrix H of the matrices B and A. H represents the coordinate correlation between A and B, that is, the correlation matrix between the position coordinates of the human body and the clothing model. The correlation matrix is decomposed to find the mapping relationship between the matrix B and the A coordinate system. The relevant calculation formula of the SVD algorithm is as follows:

$$H = \sum_{i=1}^{N} (P_A^i - C_A)(P_B^i - C_B)^T \tag{7}$$

$$|U, S, V| = SVD(H) \tag{8}$$

$$R = VU^T \tag{9}$$

$$T = -R \cdot C_B + C_A \tag{10}$$

In the formula: C_A and C_B are the center coordinates of A and B, matrix P_A^i and P_B^i represent the three-dimensional coordinate matrix of A and B. U, S, V are orthogonal matrices in the decomposition process.

B. PARTIAL TRACKING OF CLOTHING

The predicted coordinates of the local feature points are calculated by the SVD algorithm. For the local feature points
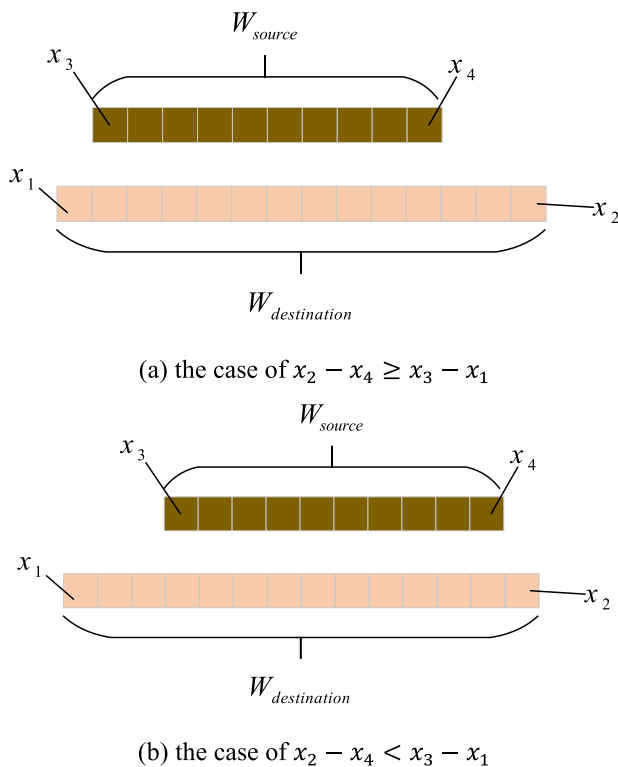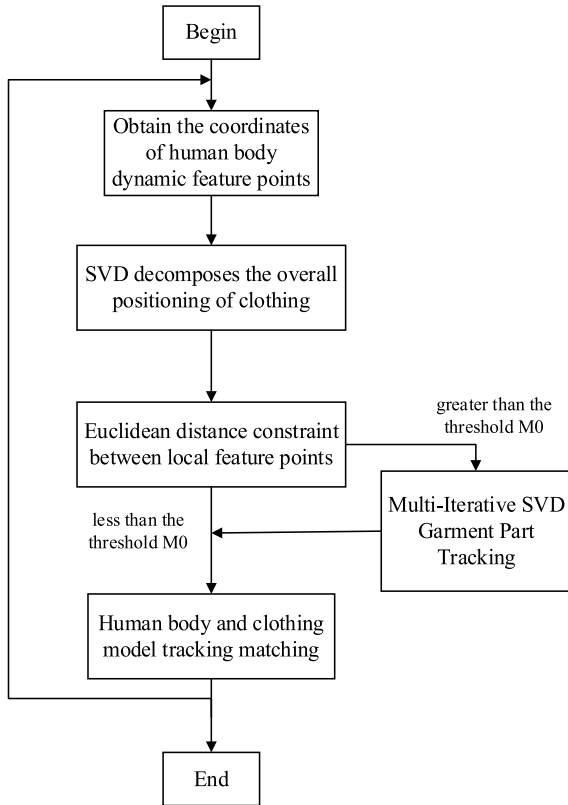
FIGURE 7. Schematic diagram of projection imaging.
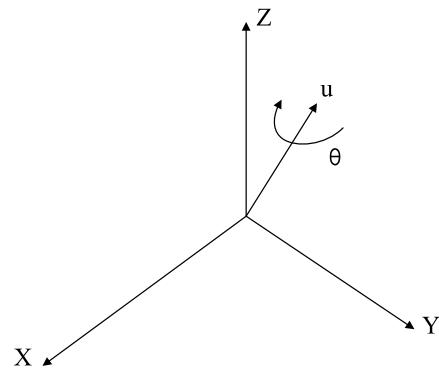
FIGURE 8. Schematic diagram of quaternion rotation.

FIGURE 6. Collaborative tracking based on GL-SVD algorithm.

with large errors, the constraint of the Euclidean distance between the skeleton points and the error threshold are used to optimize the tracking accuracy. Taking the arm joint as an example, the predicted distance between the elbow and the shoulder bone point is d_p, and the calculation formula is as follows:

$$d_p = \sqrt{(x_1 - x_2)^2 + (y_1 - y_2)^2 + (z_1 - z_2)^2} \qquad (11)$$

In the formula, (x_1, y_1, z_1) and (x_2, y_2, z_2) are the predicted coordinates of the elbow and shoulder bone points, respectively. In the same way, the real distance between the elbow and the shoulder bone point is represented by d_t, and the formula of the difference between d_p and d_t is as follows:

$$d_{(p,t)} = |d_p - d_t| \qquad (12)$$

In the formula, $d_{(p,t)}$ represents the difference between d_p and d_t.

We define the relative tracking error M, which represents the ratio of the difference between the predicted distance and the actual distance of the skeleton point and the distance before and after the skeleton point tracking. The calculation formula is as follows:

$$M = \frac{d_{(p,t)}}{d_{(t-1,t)}} \qquad (13)$$

In the formula, $d_{(t-1,t)}$ is the distance before and after the elbow bone point tracking. Set the tracking error threshold
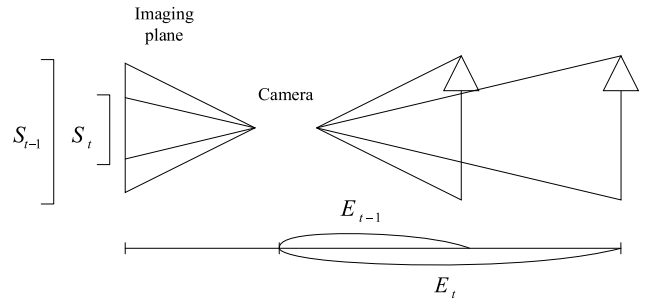
M_0, when M is greater than M_0, iteratively compute the matrices R, T to optimize the relative tracking error M.

C. ITERATIVE METHOD OF DYNAMIC FEATURE COOPERATIVE TRACKING

Figure 6 shows the dynamic feature collaborative tracking method based on the GL-SVD algorithm. Compared with the traditional SVD algorithm, the new method is based on the iterative idea of hierarchical features and has higher accuracy. By optimizing the tracking error threshold M_0, the number of iterations of the algorithm can be controlled, and the fitting accuracy and real-time performance can be balanced.

D. ITERATIVE METHOD OF DYNAMIC FEATURE COOPERATIVE TRACKING

According to the projection imaging principle shown in Figure 7, the vertical distance from the 3D object to the 2D plane maintains a certain proportional relationship with the size of the image on the 2D plane. In the figure, S_{t-1} and E_{t-1} are the human body width and depth values of the previous frame, respectively. S_t and E_t are the human body width and depth values of the current frame. In this paper, the human body depth feature I is established with a proportional relationship, as shown in the following formula:

$$I = S_{t-1} \times E_{t-1} = S_t \times E_t \qquad (14)$$

The depth value E_t is the vertical distance from the human body to the imaging plane, and the depth value data can be
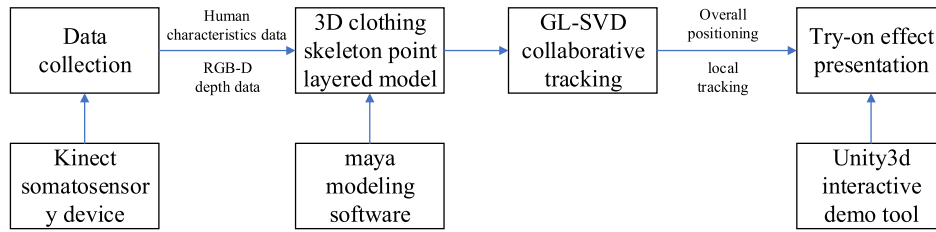
FIGURE 9. Schematic diagram of virtual clothing fitting system.

(a) 3-D Bra skirt   (b) Side leg lift   (c) Front leg lift

FIGURE 10. Clothing fitting effect of the leg-lifting posture.

obtained through Kinect perception. When the front and rear motion fields of the human body are far and near different, the size of the clothing model can be scaled by using the depth feature of the human body.

In the process of changing the posture and position of the human body, the quaternion of the matrix rotation can represent the change of the posture rotation, and the performance is stable. The quaternion q can be expressed as:

$$q = ((x, y, z) \sin \frac{\theta}{2}, \cos \frac{\theta}{2}) \qquad (15)$$

In the formula, $(x, y, z) =$u is the rotation axis of the unit vector. θ is the rotation angle, which means that a point in the three-dimensional space rotates by the angle θ around the rotation axis u of the unit vector, as shown in Figure 8.

V. EXPERIMENTS AND ANALYSIS
A. EXPERIMENTAL ENVIRONMENT CONFIGURATION
The experimental environment consists of a PC and a Kinect somatosensory device. The hardware configuration of the PC is: Windows 10 operating system, i7-9700 3.00 GHz processor, 16 GB memory, GTX 1050ti graphics card, software configuration: maya 3D modeling software, unity3d interactive demonstration tool. The frame rate of the test video is 15 frames/s. The schematic diagram of the virtual clothing fitting system designed in this paper is shown in Figure 9.

During the test, the fitter can pose or walk freely, and the video is recorded in real time by the somatosensory device. The dynamic virtual clothing fitting process changes a variety of scenarios to test the effect of the clothing fitting, including continuous replacement of actions, rapid movement back and forth, left and right, trying complex posture changes, blocking part of the body, and so on.

B. VIRTUAL CLOTHING FITTING TEST SCENE AND EFFECT COMPARISON TEST
Based on the virtual clothing fitting system designed in this paper, a comparison experiment of personalized virtual clothing fitting in various scenarios was carried out. The personalized body circumference and size data of male and female fit-testers are shown in the table 1.

Without loss of generality, the test tried a variety of styles and types of clothing models such as short-sleeved tops, sleeveless tops, long dresses, tube top skirts, trousers, cropped pants, and five-point pants. Front and back leg raises, side leg raises, T-shaped pose, arm bent pose, akimbo pose, lunge pose, and more. In view of the limited space, this paper presents the test scene as shown in Table 2, including three typical clothing types of clothing, pants, and skirts, and six human postures of different men and women. Figures 10, 11 and 12 show screenshots of the video virtual clothing fitting test effect of the algorithm in this paper.

| (a) 3-D cropped trousers | (b) Left-right lunges | (c) Forward-backward lunges |
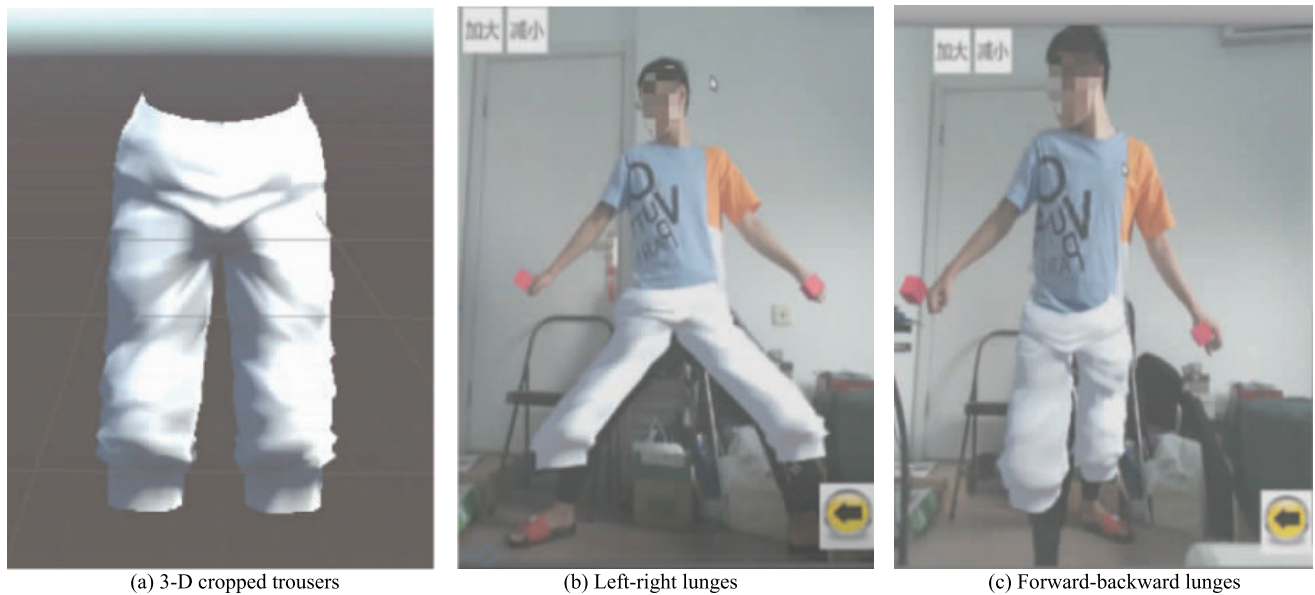
FIGURE 11. Clothing fitting effect of lunge postures.

| (a) 3-D short sleeve | (b) T-pose | (c) Side |

FIGURE 12. Clothing fitting effect of upper body postures.

The GL-SVD-based collaborative tracking method proposed in this paper can follow the changes of human pose in real time, the clothing model has a higher coverage of the body, and the applicable clothing types and human posture types are more abundant, and the dynamic clothing fitting effect test performs well.

C. EXPERIMENTAL DATA ANALYSIS

In order to preserve the figures' integrity across multiple computer platforms, we accept files in the following formats: .EPS/.PDF/.PS. All fonts must be embedded or text converted to outlines in order to achieve the best-quality results.

1) OPTIMIZING DYNAMIC TRACKING ACCURACY AND REAL-TIME PERFORMANCE

The tracking error threshold M_0 affects the accuracy and real-time performance of dynamic feature point tracking. Taking tracking the dynamic characteristics of the wrist as an example, by conducting comparative experiments on the threshold M_0 in 6 groups, the average error and iteration time of 10 tracking processes are taken as the average value of each group of experiments. Figure 13 shows the results of relative tracking error and iterative computation time as a function of the threshold M_0, respectively.

According to the figure, M increases with the increase of M_0, and T decreases with the increase of M_0. In order

TABLE 2. Personalized human circumference feature.

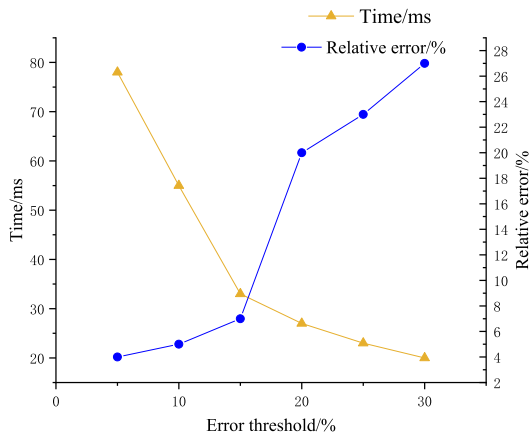| Scene number	Figure sequence	Perspective	Attitude	Clothing type
1	Figure 10(b)	Front	Side leg lift	Tube top dress
2	Figure 10(c)	Front	Front leg lift	Tube top dress
3	Figure 11(b)	Front	Lunge left and right	Cropped pants
4	Figure 11(c)	Front	Front and rear lunges	Cropped pants
5	Figure 12(b)	Front	T-shaped	Short sleeve
6	Figure 12(c)	Side	Stand	Short sleeve

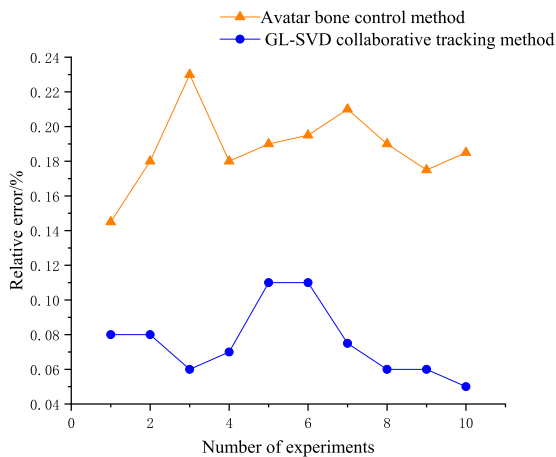**FIGURE 13.** Tracking accuracy and real-time analysis.

FIGURE 14. Tracking accuracy comparison.

to ensure high precision and less iteration time, the tracking error threshold $M\_0=15\%$ is taken as the optimal value.

2) ACCURACY COMPARISON OF HUMAN BODY DYNAMIC TRACKING

Taking the dynamic tracking accuracy of human torso feature points as an example, the GL-SVD-based collaborative tracking method proposed in this paper is compared with the avatar skeleton control method, and the results are shown in Figure 14.

The research shows that, compared with the Avatar method, the GL-SVD-based collaborative tracking method proposed in this paper reduces the relative tracking error M by about 10%, and the tracking accuracy can be significantly improved. It has the advantages of fast and accurate performance, so it can ensure the dynamic tracking of clothing models The real-time and precision requirements of the virtual machine have improved the real experience of virtual clothing fitting.

VI. CONCLUSION
In this paper, a 3D clothing skeleton hierarchical model for human dynamic feature tracking is proposed to distinguish the motion features of different parts of the human body, and a collaborative tracking method based on the global-local iterative GL-SVD algorithm is designed to hierarchically control 3D clothing skeletons. model, so as to realize the dynamic tracking and fitting of human body posture. Based on the Kinect somatosensory video interactive environment, through the test and performance comparison of various virtual clothing fitting scenarios, the new 3D dynamic virtual clothing fitting technology reduces the relative tracking error by more than 10%, and can achieve real-time and dynamic clothing fitting effect, which is significantly improved It can be applied to a variety of clothing types and continuous dynamic changes in human posture, and has certain generality and robustness. In the future, we will try to study more complex clothing styles to promote the application and development of low-cost 3D virtual clothing fitting intelligent systems.

REFERENCES
[1] C. M. Armstrong, K. Niinimäki, C. Lang, and S. Kujala, "A use-oriented clothing economy? Preliminary affirmation for sustainable clothing consumption alternatives," *Sustain. Develop.*, vol. 24, no. 1, pp. 18–31, Jan. 2016.
[2] A. T. Asbeck, S. M. M. De Rossi, I. Galiana, Y. Ding, and C. J. Walsh, "Stronger, smarter, softer: Next-generation wearable robots," *IEEE Robot. Autom. Mag.*, vol. 21, no. 4, pp. 22–33, Dec. 2014.
[3] S. Cakmak, N. Y. Cegindir, and H. G. Yilmaz, "The development of posture supporting soft exosuit design for adolescent idiopathic scoliosis," *Int. J. Clothing Sci. Technol.*, vol. 34, no. 2, pp. 228–240, Mar. 2022.
[4] A. P. C. Chan, Y. P. Guo, F. K. W. Wong, Y. Li, S. Sun, and X. Han, "The development of anti-heat stress clothing for construction workers in hot and humid weather," *Ergonomics*, vol. 59, no. 4, pp. 479–495, Apr. 2016.
[5] Y. M. Choo and Y. E. Yo, "A study on the development model for personalized men's suit untact service," *J. Cultural Product Des.*, vol. 63, pp. 83–95, Jan. 2020.

[6] K.-Y. Chung, Y.-J. Na, and J.-H. Lee, "Interactive design recommendation using sensor based smart wear and weather WebBot," *Wireless Pers. Commun.*, vol. 73, no. 2, pp. 243–256, Nov. 2013.

[7] I. Ciesielska-Wrobel, E. Denhartog, and R. Barker, "The influence of designs of protective uniforms on firefighters' performance during moderate physical exercises," *Textile Res. J.*, vol. 88, no. 17, pp. 1979–1991, 2018.

[8] I. Cucchi, A. Boschi, C. Arosio, F. Bertini, G. Freddi, and M. Catellani, "Bio-based conductive composites: Preparation and properties of polypyrrole (PPy)-coated silk fabrics," *Synth. Met.*, vol. 159, nos. 3–4, pp. 246–253, Feb. 2009.

[9] P. Escobedo, J. de Pablos-Florido, M. A. Carvajal, A. Martínez-Olmos, L. F. Capitán-Vallvey, and A. J. Palma, "The effect of bending on laser-cut electro-textile inductors and capacitors attached on denim as wearable structures," *Textile Res. J.*, vol. 90, nos. 21–22, pp. 2355–2366, Nov. 2020.

[10] K. H. Foysal, H.-J. Chang, F. Bruess, and J.-W. Chong, "Body size measurement using a smartphone," *Electronics*, vol. 10, no. 11, p. 1338, Jun. 2021.

[11] G. Goncu-Berk and B. G. Tuna, "The effect of sleeve pattern and fit on e-textile electromyography (EMG) electrode performance in smart clothing design," *Sensors*, vol. 21, no. 16, p. 5621, 2021.

[12] R. Granberry, K. Eschen, B. Holschuh, and J. Abel, "Functionally graded knitted actuators with NiTi-based shape memory alloys for topographically self-fitting wearables," *Adv. Mater. Technol.*, vol. 4, no. 11, Nov. 2019, Art. no. 1900548.

[13] C. Guan, S. Qin, W. Ling, and G. Ding, "Apparel recommendation system evolution: An empirical review," *Int. J. Clothing Sci. Technol.*, vol. 28, no. 6, pp. 854–879, Nov. 2016.

[14] Y. Guo, A. P. Chan, F. K. Wong, Y. Li, S. Sun, and X. Han, "Developing a hybrid cooling vest for combating heat stress in the construction industry," *Textile Res. J.*, vol. 89, no. 3, pp. 254–269, Feb. 2019.

[15] J. Han, W. Song, A. Gozho, Y. Sung, S. Ji, L. Song, L. Wen, and Q. Zhang, "LoRa-based smart IoT application for smart city: An example of human posture detection," *Wireless Commun. Mobile Comput.*, vol. 2020, pp. 1–15, Aug. 2020.

[16] H. Harms, O. Amft, and G. Tröster, "Estimating posture-recognition performance in sensing garments using geometric wrinkle modeling," *IEEE Trans. Inf. Technol. Biomed.*, vol. 14, no. 6, pp. 1436–1445, Nov. 2010.

[17] C. He, S. Korposh, F. U. Hernandez, L. Liu, R. Correia, B. R. Hayes-Gill, and S. P. Morgan, "Real-time humidity measurement during sports activity using optical fibre sensing," *Sensors*, vol. 20, no. 7, p. 1904, Mar. 2020.

[18] H. A. Horst, C. Baylosis, and S. Mohammid, "Looking professional: How women decide what to wear with and through automated technologies," *Converg. Int. J. Res. New Media Technol.*, vol. 27, no. 5, pp. 1250–1263, 2021.

[19] K. Joyce, "Smart textiles: Transforming the practice of medicalisation and health care," *Sociol. Health Illness*, vol. 41, no. S1, pp. 147–161, Oct. 2019.

[20] J. Kim, J. Kim, D. Lee, and K.-Y. Chung, "Ontology driven interactive healthcare with wearable sensors," *Multimedia Tools Appl.*, vol. 71, no. 2, pp. 827–841, Jul. 2014.

[21] J. S. Ko, "A study on problems and solutions of fire service for chemical substance terrorism," *Korean Terrorism Studies Rev.*, vol. 6, no. 4, pp. 22–51, 2013.

[22] G. McAllister, S. J. McKenna, and I. W. Ricketts, "Hand tracking for behaviour understanding," *Image Vis. Comput.*, vol. 20, no. 12, pp. 827–840, Oct. 2002.

[23] M. R. Talebpour, O. Sahin, R. Siems, and R. A. Stewart, "Water and energy Nexus of residential rainwater tanks at an end use level: Case of Australia," *Energy Buildings*, vol. 80, pp. 195–207, Sep. 2014.

[24] L. Xu, K. Du, Y. Liu, K. Xie, H. Tang, and C. Zhang, "The fabrication and properties of a flexible sensor based on polyvinylidene fluoride fiber," *Textile Res. J.*, vol. 92, nos. 19–20, pp. 3443–3450, Oct. 2022.

[25] L. Zhao, S. Liu, and X. Zhao, "Big data and digital design models for fashion design," *J. Engineered Fibers Fabrics*, vol. 16, Jan. 2021, Art. no. 155892502110190.

HUAPING ZHU was born in Hunan, China, in 1977. She received the bachelor's degree from Hunan Normal University, in 1999, and the master's degree from Zhejiang University of Science and Technology, in 2013. She was with Guangxi Textile Industry School, from 2001 to 2018, and Nanning Normal University, from 2018 to 2023. She is currently with Nanning Normal University. She published seven articles and three series of works. Her research interests include big data and machine learning. She has won the National Teaching Achievement Award, District level Teaching Achievement Special Award, and Second Prize.

TAO ZHANG was born in Hebei, China, in 1978. He studied from Hebei University of Science and Technology, from 1998 to 2002, and received the bachelor's degree, in 2022. From 2002 to 2023, he worked in software development in Shenzhen. During this period, a total of three software copyrights and one invention patent were produced. His research interests include big data and software engineering.

FEN WANG was born in Changsha, China, in 1979. She received the master's degree from Sehan University, South Korea. She is currently with the College of Humanities, Arts and Design, Guangxi University of Science and Technology. Her research interests include computer vision and intelligent computing.

• • •